EPJ Web of Conferences **146**, 04042 (2017) DOI: 10.1051/epjconf/201714604042
ND2016

Fission-fragment total kinetic energy and mass yields for neutron-induced fission of ^{235}U and ^{238}U with E_n =200 keV – 30 MeV

D.L. Duke[1,a], F. Tovesson[1], T. Brys[2], V. Geppert-Kleinrath[1], F.-J. Hambsch[2], A. Laptev[1], R. Meharchand[3], B. Manning[1], D. Mayorov[1], K. Meierbachtol[1], S. Mosby[1], B. Perdue[4], D. Richman[5], D. Shields[6], and M. Vidali[2]

[1] Los Alamos National Laboratory, PO Box 1663, Los Alamos, NM, USA
[2] Joint Research Center, Retieseweg 111, 2440 Geel, Belgium
[3] Institute for Defense Analyses, 4850 Mark Center Dr., Alexandria, VA, USA
[4] Commonwealth Computer Research, Inc., 1440 Sachem Pl., Charlottesville, VA, USA
[5] Michigan State University, 220 Trowbridge Rd., East Lansing, MI, USA
[6] Colorado School of Mines, 1500 Illinois St., Golden, CO, USA

Abstract. The average Total Kinetic Energy ($\overline{TKE}$) release and fission-fragment yields in neutron-induced fission of ^{235}U and ^{238}U was measured using a Frisch-gridded ionization chamber. These observables are important nuclear data quantites that are relevant to applications and for informing the next generation of fission models. The measurements were performed a the Los Alamos Neutron Science Center and cover $E_n = 200$ keV – 30 MeV. The double-energy (2E) method was used to determine the fission-fragment yields and two methods of correcting for prompt-neutron emission were explored. The results of this study are correlated mass and $\overline{TKE}$ data.

1. Introduction

Most of the energy released during the fission process is in the form of the kinetic energy of the fission fragments. Many fission observables, such as the average total kinetic energy ($\overline{TKE}$) and the mass of the fission fragments, evolve with the excitation energy of the compound nucleus. Despite decades of fission research, measurements of $\overline{TKE}$ and mass yields as a function of excitation energy are sparse for the major and minor actinides. In this work, we provide a correlated measurement of $\overline{TKE}$ and mass yields for neutron induced fission with neutron energies E_n = 200 keV – 30 MeV for ^{235}U and ^{238}U. This measurement was performed using a Frisch-gridded ionization chamber as part of a program at Los Alamos National Laboratory to provide $\overline{TKE}$ measurements for a host of fissionable isotopes relevant to energy and defense applications. The additional data will be used to test and inform current fission models.

Previous data is available for ^{235}U, however these measurements were performed for $E_n \leq 9$ MeV [1] and recent measurements are subject to large uncertainties [2]. For ^{238}U, measurements exist for $E_n \leq 6$ MeV [3,4] and one measurement exists at high energy $E_n = 1$–400 MeV [5]. These data were used in semi-emperical fission models by Madland [1] for ^{235}U, ^{238}U, and ^{239}Pu. These models were extended by Lestone and Strother [6] to include multi-chance fission thresholds. Further systematic study of these isotopes is necessary to test fission models. Very little data exists on fission-fragment mass yields at neutron energies other than at $E_n =$ thermal or 14 MeV [7].

2. Experiment

2.1. Neutron source

The experiments were carried out at the Los Alamos Neutron Science Center – Weapons Neutron Research (LANSCE – WNR), an 800 MeV proton accelerator incident on an unmoderated tungsten spallation target [8]. The 90 L flightpath was used, which has a neutron flux with energies spanning hundred's of keV up to hundred's of MeV. The neutron energies were determined using a time-of-flight method.

2.2. Detector

A Frisch-gridded ionization chamber (FGIC) was used to make the measurements because of its good intrinsic energy resolution of 0.5 – 1.0% and high efficiency [9]. The detector has a center cathode plane where the thin actinide target was mounted and Frisch grids and anodes on both halves of the detector volume. The detector layout is schematically shown in Fig. 1. The volume is about 1 L and holds a fill gas of P-10, 90% argon with 10% isobutane. With this detector, the angle and energy of the

[a] e-mail: dlduke@lanl.gov

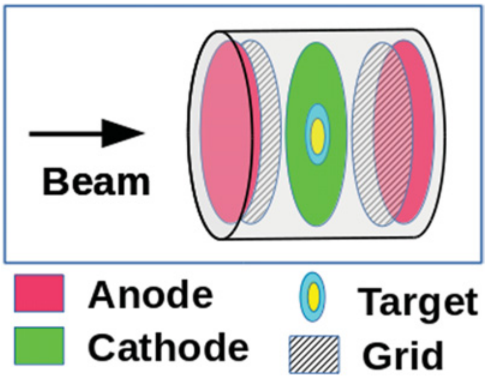

Figure 1. A cartoon of the detector components the target is on the center cathode (green), with fragments extending into volums towards the grids (lined) and anodes (pink).

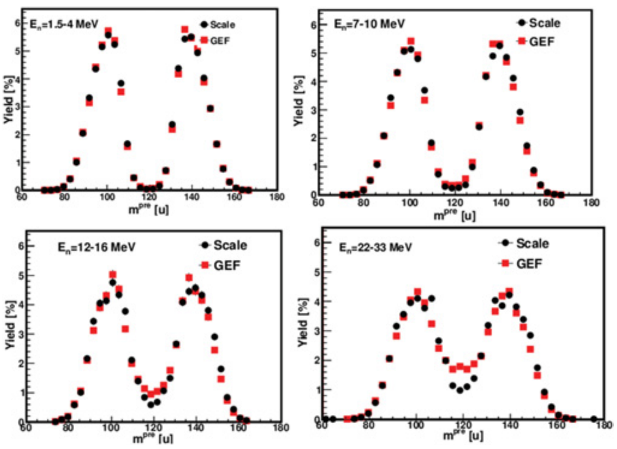

Figure 2. Mass yields for ^{238}U pre-prompt neutron emission corrected using the 2E analysis comparing method 1 (“scale”) and method 2 (GEF). The underrepresentation in the symmetric region is most clear in the $E_n = 22 - 33$ MeV region.

two fission fragments can be measured. The FGIC and a digital data acquisition system developed for these studies is described in detail in Ref. [10].

3. Analysis

An analysis procedure known as the double-energy or “2E” method is employed. Using conservation of energy, momentum, and nucleon number, the masses of the fission fragments can be determined with 4–5 amu resolution while correcting the data for mass-dependent effects. The process is described in detail in [11] and [12].

While calculating the masses of the fission products, a correction is required for prompt neutron emission during fission. Multiple models exist for the average number of prompt neutrons emitted as a function of fragment mass, however very few measurements exist, especially for fast neutron-induced fissioning systems. During the analysis of this data, two models were compared to correct for prompt neutron emission. Method 1 is based on scaling the thermal measurement of $\nu(A)$ up for higher excitation energies, while keeping the integral equal to the total number of neutrons emitted, $\bar{\nu}$. It assumes that the number of neutrons evaporated off the fragments is scaled-up equally between the 2 fragments [13]. Method 2 assumes that the heavy fragment evaporates more neutrons at higher energies and is based on simulations at each neutron energy using the GEF code [14]. The resulting mass distributions from the two methods are shown for comparisson in Fig. 2. For the final calculations, method 2 was chosen because it better reproduced the symmetric fission component on the mass distributions for $m = 110 - 120$ u at $E_n = 14$ MeV compared to evaluation [7]. Method 1 overcompensates for shell structure at $m = 132$ u and results in an underrepresented symmetric fission component.

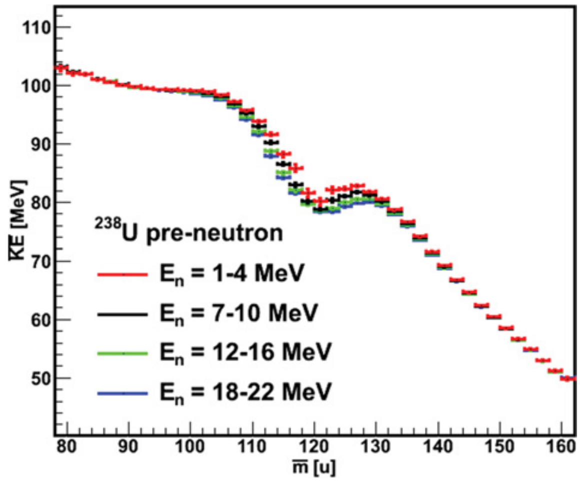

Figure 3. The average kinetic energy per fragment mass in ^{238}U. Error bars are statistical.

4. Results

The correlated mass and kinetic energy infomation can be compared in a variety of ways to understand how the energy is partitioned in the fissioning system. The complete $\overline{TKE}$ evolution with E_n can be found in Ref. [11] and [12]. Because of the 4-5 u resolution of the detector, the data presented there is smoothed to 4 u resolution. Figure 3 shows the average kinetic energy given a fragment mass in ^{238}U. The kinetic energy of heavy ($m \geq 135$ u) and light ($m \leq 100$ u) fragments is stable with increasing excitation energy. A slight decrease in average kinetic energy occurs for more symmetric fragments with increasing E_n.

Figure 4 illustrates correlation of total kinetic energy with mass for the heavy fragment. It shows that the growing symmetric fission component masses ($m = 120 - 125$ u) generally have lower TKE which in part accounts for the decreasing trend in $\overline{TKE}$ with E_n.

5. Conclusion

The high efficiency of the FGIC allows the general trends in fission observables to be measured over a broad range of excitation energies. Future studies will focus on measuring fission fragment masses and energies for other elements and uranium isotopes. To fully take advantage of FGIC + 2E style experiments to measure energy-dependent trends in correlated fission observables, this work demonstrates the need for measurements of mass-dependent prompt

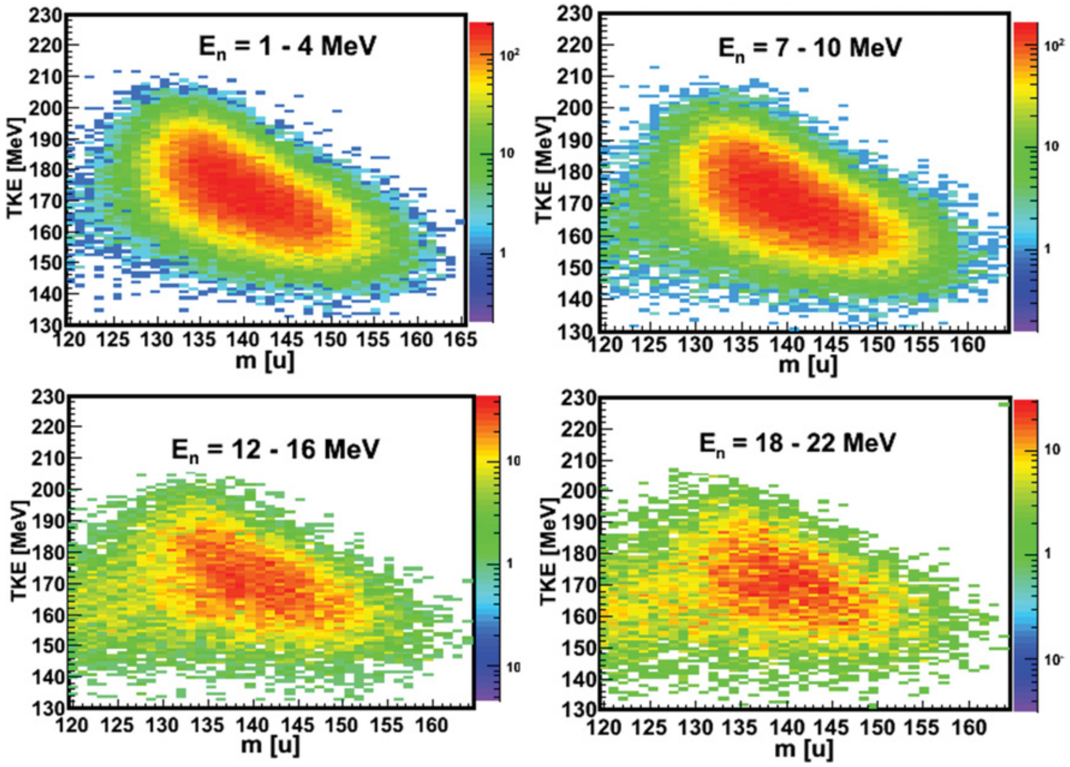

Figure 4. The TKE as a function of heavy fragment mass for ^{238}U. The color scale goes with the yield.

neutron emission at high excitation energy to make more accurate corrections to the data.

References

[1] D. Madland, Nuclear Physics A **772**, 113 (2006)
[2] R. Yanez, L. Yao, J. King, W. Loveland, F. Tovesson, N. Fotiades, Phys. Rev. C **89**, 051604 (2014)
[3] F. Vivès, Ph.D. thesis, L'Universite Bordeaux I (1998)
[4] E. Birgersson, A. Oberstedt, S. Oberstedt, F.J. Hambsch, Nuclear Physics A **817**, 1 (2009)
[5] C. Zöller, Ph.D. thesis, Technische Hochschule Darmstadt (1995), `http://www-win.gsi.de/charms/data.htm`
[6] J. Lestone, T. Strother, Nuclear Data Sheets **118**(0), 208 (2014)
[7] T.R. England, B.F. Rider, Tech. rep., Los Alamos National Laboratory (October 1994), `http://ie.lbl.gov/fission/endf349.pdf`
[8] P. Lisowski, C. Bowman, G. Russel, S. Wender, Nuclear Science and Engineering **106**(2), 208 (1990)
[9] C. Budtz-Jørgensen, H.H. Knitter, C. Straede, F.J. Hambsch, R. Vogt, Nuclear Instruments and Methods in Physics Research Section A: Accelerators, Spectrometers, Detectors and Associated Equipment **258**(2), 209 (1987)
[10] S. Mosby, F. Tovesson, A. Couture, D. Duke, V. Kleinrath, R. Meharchand, K. Meierbachtol, J. O'Donnell, B. Perdue, D. Richman et al., Nuclear Instruments and Methods in Physics Research Section A: Accelerators, Spectrometers, Detectors and Associated Equipment **757**, 75 (2014)
[11] D. Duke, Ph.D. thesis, Colorado School of Mines (2015)
[12] D. Duke, F. Tovesson, T. Brys, F.J. Hambsch, A. Laptev, S. Mosby, M. Vidali, Phys. Rev. C, In press (2016)
[13] J. Lestone, Nuclear Data Sheets **112**, 3120 (2011), special Issue on ENDF/B-VII.1 Library
[14] B. Jurado, K.H. Schmidt, *A General Description of Fission Observables (GEF), version 2015/1.1* (2015), `http://www.khs-erzhausen.de/GEF.html`